

## Material transport from marker tiles in the JET divertor

J. Likonen<sup>a,\*</sup>, J.P. Coad<sup>b</sup>, E. Alves<sup>c</sup>, N. Catarino<sup>c</sup>, I. Coffey<sup>b</sup>, S. Krat<sup>d,e</sup>, M. Mayer<sup>d</sup>,  
K. Mizohata<sup>f</sup>, A. Widdowson<sup>b</sup>

<sup>a</sup> VTT Technical Research Centre of Finland, PO Box 1000, FIN-02044 VTT, Finland

<sup>b</sup> Culham Centre for Fusion Energy, Culham Science Centre, Abingdon, Oxon OX14 3DB, UK

<sup>c</sup> IPFN, Instituto Superior Tecnico, Universidade de Lisboa, 1049-001 Lisboa, Portugal

<sup>d</sup> Max Planck Institute for Plasma Physics, Boltzmannstr. 2, 85748 Garching, Germany

<sup>e</sup> National Research Nuclear University MEPhI, Moscow, Russia

<sup>f</sup> University of Helsinki, Department of Physics, PO Box 64, FI-00014 University of Helsinki, Finland

### ABSTRACT

For each of the three JET ILW campaigns a few special marker tiles were placed in the divertor. Amongst the W-coated CFC tiles are tiles coated with a  $\sim 3 \mu\text{m}$  layer of Mo with a  $\sim 4 \mu\text{m}$  topcoat of W and tiles with just a  $\sim 4 \mu\text{m}$  layer of Mo to measure erosion and re-deposition.

During ILW1 just one Mo marker tile was included in the inner divertor band of Tiles 3. After ILW1 the Mo marker was removed for analysis and *inter alia* two W-coated Tiles 4 to check for re-deposited Mo. About 7% of the Mo removed from the Tile 3 Mo marker was found on band 4 tiles.

A fresh Mo marker Tile 3 was inserted in for ILW2 + 3 plus a Mo marker Tile 4 for ILW2 (after which it was removed for analysis). Tile 4 removed after ILW3 was measured for Mo re-deposition. The Mo deposition pattern on Tile 4 with a regular W topcoat was quite different to that after ILW1, with much more Mo located towards the corner of the divertor.

### Introduction

During every shutdown of the Joint European Tokamak (JET), tiles and other components are removed from the plasma-facing surfaces to analyse their surfaces (and are replaced with new components) [1–3]. These analyses give information on deposition onto the surfaces during the period of exposure and in some cases on the erosion from these surfaces so that a picture can be assembled of transport of material by the plasma within the tokamak. For example, much of the main wall inside JET is covered with beryllium (Be) tiles whereas the plasma-facing surfaces of the divertor are tungsten (W), and the transfer of Be from the main chamber onto the divertor can be assessed [1,2]. To study the movement of material within the divertor some special marker tiles have been installed. The JET ITER-like Wall (ILW) divertor mostly consists of carbon fibre composites (CFC) tiles coated with a  $\sim 20 \mu\text{m}$  thick W layer over a thin molybdenum (Mo) interlayer designed to inhibit interaction between the C and the W. Some poloidal sets of tiles have the outer  $12 \mu\text{m}$  of the W replaced by  $4 \mu\text{m}$  of Mo plus  $4 \mu\text{m}$  of W on top to act as erosion/deposition markers during ILW campaigns: deposition on the tile is clearly measured, whilst erosion of up to  $4 \mu\text{m}$  is seen as thinning of the top W layer. Furthermore, a few of the marker tiles only have the  $4 \mu\text{m}$  Mo coating to facilitate transport studies of Mo and W

within the divertor. During the first ILW campaign (ILW1 from 2011 to 2013) one Mo-only marker tile was installed – a Tile 3 from the lower part of the inner divertor wall (see Fig. 1a-b) - full positional designation 14ING3B (module 14 (Narrow), Inner wall, tile position 3B) which was removed during the subsequent shutdown. This facilitated detection of W from surrounding tiles onto this tile and of Mo migration onto other tiles in the divertor, specifically to Tiles 14BNG4D and 2BNG4C (innermost base Tiles 4 with standard Mo + W markers) which were also removed for extensive study.

A fresh Mo marker tile was placed at 14ING3B for ILW2 (2013–2014) and ILW3 (2015–2016) and a second Mo marker was installed at position 2BNG4C just for ILW2 before being exchanged for a standard W-coated tile. As usual, further tiles were removed for detailed analysis after ILW3.

### Experimental

All the divertor marker tiles were measured before mounting in JET by the Ion Beam Analysis (IBA) technique Rutherford Back-scattering (RBS) using 3 MeV protons [3]. Deposition of W on Mo markers was measured by RBS using  $^4\text{He}$ . Deposition of Mo on W-coated tiles was measured using Secondary Ion Mass Spectrometry (SIMS) using a 5 keV

\* Corresponding author.

E-mail address: [jari.likonen@vtt.fi](mailto:jari.likonen@vtt.fi) (J. Likonen).

<https://doi.org/10.1016/j.nme.2023.101505>

Received 26 June 2023; Received in revised form 29 August 2023; Accepted 8 September 2023

Available online 9 September 2023

2352-1791/© 2023 The Authors. Published by Elsevier Ltd. This is an open access article under the CC BY-NC-ND license (<http://creativecommons.org/licenses/by-nc-nd/4.0/>).

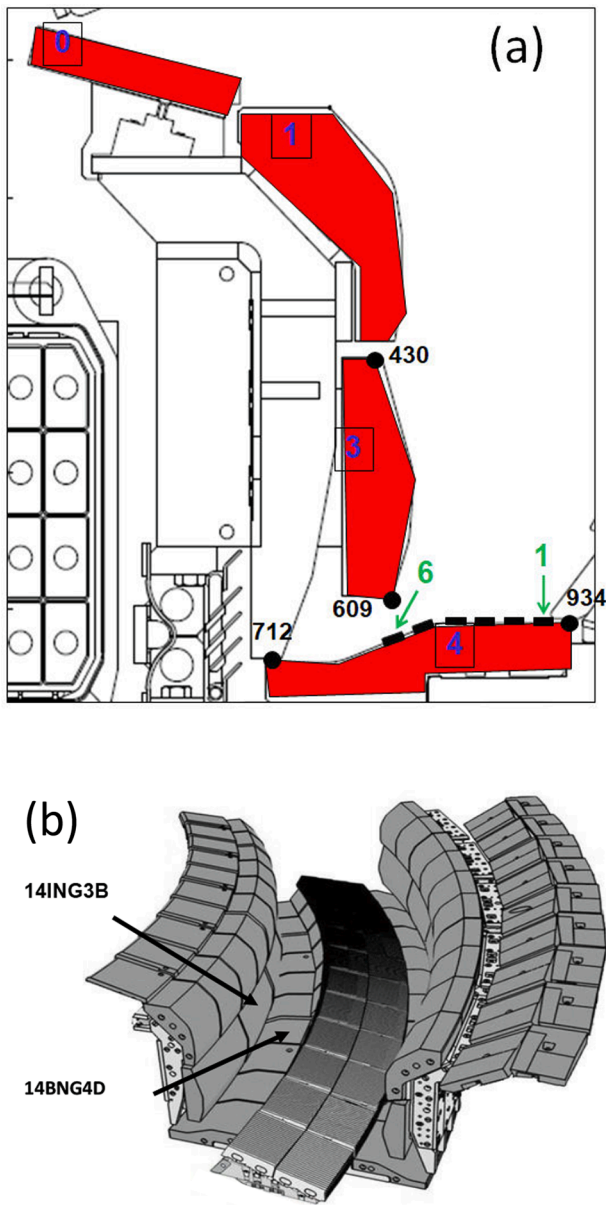


**Fig. 1.** (a) Sample locations (in green) on Tile 4 and (b) 3D geometry of divertor. Analysed Tiles 14ING3B and 14BNG4D in module 14 are indicated. S-coordinate is the distance around the divertor surface in millimetres. Origin of the S-coordinate is at the left edge of Tile 0. S-coordinates (in black) for the tiles are given in a.

$O_2^+$  beam [4] and by Time-of-flight Elastic Recoil Detection Analysis (TOF-ERDA) using a 50 MeV  $^{127}I$  beam. The depth of analysis by TOF ERDA is  $\sim 180$  nm, whilst SIMS profiles into the surface in a continuous manner but is calibrated against the TOF ERDA for the equivalent depth at the surface. Cylindrical samples with a diameter of 17 mm were cut from the divertor tiles using a hollow drill.

A variety of plasma configurations are employed at JET, however during ILW1 the majority of pulses used the V5 configuration shown in Fig. 2 so that the inner strike point (ISP) was most commonly near the top of Tile 3 with the outer strike point (OSP) on Tile 5 (which is a set of solid W blocks), and this is further illustrated in Fig. 3 which gives the integrated times at each position on Tiles 1, 3 and 4. During ILW2 and ILW3 the ISP was, however, mainly on Tile 3 or on the top sloping part of Tile 4 (configuration HT).

## Results and discussion

By comparing the RBS measurements from before and after exposure during ILW1 it can be seen there was Mo erosion from Tile 14ING3B after the first ILW campaign (ILW1) whilst in contrast there was some deposition of W on the tile, as shown in Fig. 4. Both the Mo erosion and the W deposition are greatest towards the top of the tile, whereas the ISP was located nearer the centre of the tile, but the average amount of re-deposition visible at the bottom of the tile, but the average amount of net Mo erosion across the tile was  $6.8 \times 10^{18} \text{ cm}^{-2}$ . Tokitani et al [5] show that the surface of the coating is micro-rough and that each “hill” is a net erosion zone whilst the associated “valley” and downward slope in the shadow of the field line direction can accumulate W and other deposition - the field line direction typical for this location in the V5 configuration is  $\sim 2$ -3 degrees to the surface [5].

Metallic elements are principally eroded by incident plasma ions as atoms or ions, and return to the surface a short distance farther along the plasma field line direction where they may be re-eroded: migration may thus occur by a series of “hops”. Migration of W was observed onto the Mo marker Tile 14ING3B from toroidally adjacent W-coated tiles and from the row of Tiles 1 poloidally above Tile 3. Although the re-deposited W is greatest towards the top of the tile where the Mo erosion is also greatest, the Mo would be preferentially sputtered as it is more easily eroded by deuterium ions ( $\sim \times 5$  for 200 eV ions [6,7]). As the incident plasma ions have both toroidal and poloidal components, the eroded Mo may migrate toroidally to an adjacent Tile 3 or poloidally down onto Tile 4. Material is sputtered from the surface predominantly as a neutral atom but is then ionised and can travel in the direction of the field lines. As the B-field is at an angle of 2.2 degrees to the horizontal (toroidal) direction and the height of a Tile 3 is 18 cm, the distance to traverse is 470 cm. Thus, an ion born at the top of a Tile 3 might travel up to 470 cm before reaching the bottom of the Tiles 3, whereas, an atom eroded from near the bottom of Tile 3 will have a greater probability of reaching a Tile 4.

Analysis of Tiles 4 by SIMS (as normalised using TOF ERDA data) after the ILW1 and ILW3 campaign revealed significant amounts of Mo had been transferred to 14BNG4D. Locations within the divertor are given as s-coordinates, which are distances around the divertor surface in millimetres starting from the left edge of Tile 0, and the s-coordinates (in black) for these tiles were given in Fig. 1a. Fig. 5 shows the SIMS depth profiles for a sample taken at  $s \sim 810$  mm from each of the ILW1 and ILW2 + 3 Tiles 4. Mo has a distinct surface peak which extends to a depth of  $\sim 2 \mu\text{m}$  in the case of the ILW1 sample and to a depth of  $\sim 4 \mu\text{m}$  in the case of the ILW2 + 3 sample, respectively. The surface peak for Mo in the case of the ILW2 + 3 sample is clearly higher than that for the ILW1 sample. As discussed earlier, the SIMS Mo signal was normalised to TOF-ERDA up to a depth of  $\sim 180$  nm and the total deposited Mo amount was obtained by integrating the Mo signal up to depths of  $\sim 2 \mu\text{m}$  (ILW1) and  $\sim 4 \mu\text{m}$  (ILW2 + 3). Fig. 6 shows that following ILW1 Mo was located mainly towards the top of the tile (s-coordinates  $\sim 800$ - $900$  mm). Furthermore, almost identical amounts of Mo were found on Tile 2BNG4C, which had been on the opposite side of the torus,  $\sim 770$  cm away toroidally, indicating that the Mo can travel long distances. However, the amount of deposited Mo only averaged  $\sim 4 \times 10^{15} \text{ cm}^{-2}$  so even though the Tile 4 area was greater than the single Tile 3, it only represented  $\sim 7\%$  of the Mo eroded - the rest may be assumed to be re-deposited on the other Tiles 3 that were not available for post-mortem surface analyses.

The new Tile 14BNG4D inserted after ILW1 was removed after ILW2 and 3 and was analysed by SIMS across two different scans (separated by  $\sim 10$  cm toroidally) which gave very similar results. However, the profiles at this time were different to that after ILW1, increasing by three orders of magnitude from  $s = 925$  mm to  $s = 780$  mm (Fig. 6). Although there was again a Mo marker tile at 14ING3B during this time, there had also been a Mo marker tile at 2BNG4C for ILW2 and there had also been Laser Blow Off (LBO) experiments [8] using Mo early in ILW2 and

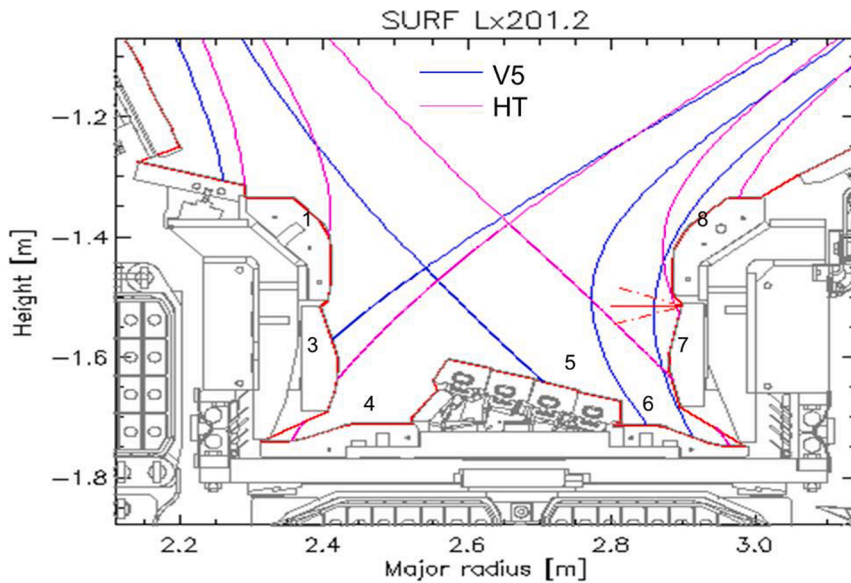


Fig. 2. Typical plasma configurations during ILW1 and ILW2-ILW3.

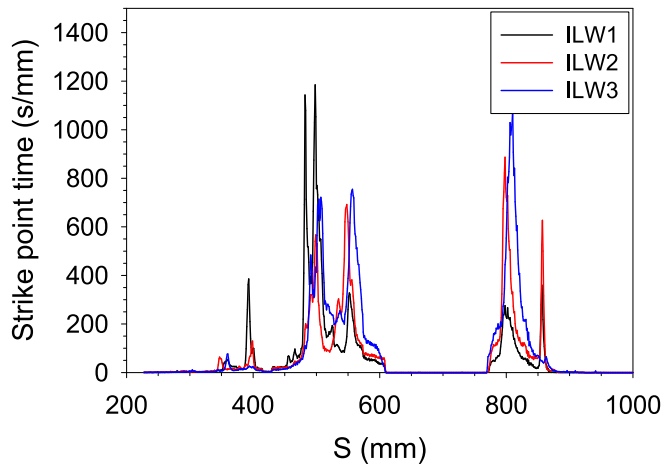


Fig. 3. Integrated times for the inner strike point position on Tiles 1, 3 and 4.

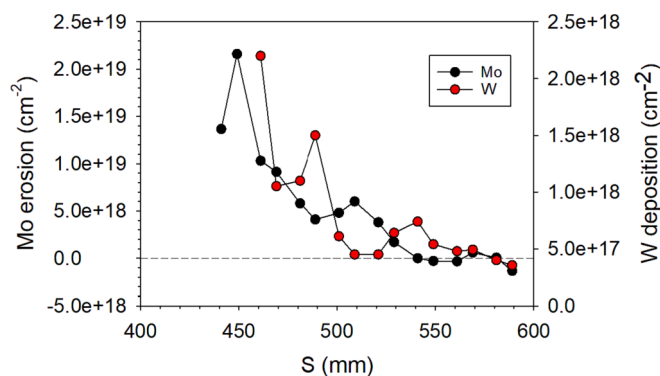


Fig. 4. Amounts of Mo erosion and W deposition measured by RBS on Tile 14ING3B after exposure during ILW1.

towards the end of ILW3. LBO involves firing a laser at a Mo film being held at a crucible at a Main Horizontal Port (at the outer midplane - OMP) at Octant 6 during a plasma pulse. There had been LBO experiments during ILW1, but these did not involve Mo. Contributions to the

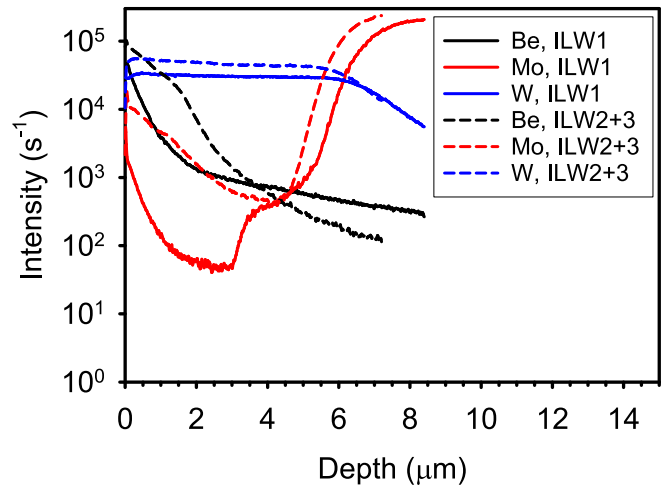


Fig. 5. SIMS depth profiles for ILW1 (solid lines) and ILW2 + 3 (dashed lines) sample 4 (s ~ 810 mm) on Tile 4.

Mo deposition on 14BNG4D may have resulted from each of these sources: Re-deposition from 14ING3B, re-deposition from 2BNG4C or deposition resulting from LBO. Re-deposition from 14ING3B may be assumed to be similar in location but significantly reduced to that following ILW1 as the strike point was much less frequently on that tile. Material sputtered from 2BNG4C can only re-deposit onto other Tiles 4 and is likely to migrate towards the inner corner which has been a sink for plasma impurities for all JET Mk II divertors – as examples Be, C and D all peak strongly at about  $s = 780$  mm [1,2], whilst the peak of W deposition on 2BNG4C itself is at the same location [3]. The mean net erosion from 2BNG4C during ILW2 was  $10^{18} \text{ cm}^{-2}$  [3] and the total erosion source from the tile was  $\sim 3 \times 10^{20} \text{ cm}^{-2}$  Mo atoms, requiring a mean re-deposit of  $\sim 10^{16} \text{ cm}^{-2}$  over the 95 other Tiles 4, which is consistent with the data in Fig. 6. Deposition of Mo resulting from LBO is possible; each ablation releases  $\sim 1018$  atoms, of which  $\sim 2 \times 10^{17}$  are estimated to enter the plasma [9]. During ILW2 and 3 there were a total of 36 Mo ablations, giving a possible source of  $\sim 7 \times 10^{18}$  atoms. However, deposition onto Tiles 4 either requires transport around the plasma boundary all the way from the OMP to the inner divertor corner (and requiring discharges with the ISP on Tile 4 to avoid plating out en route),

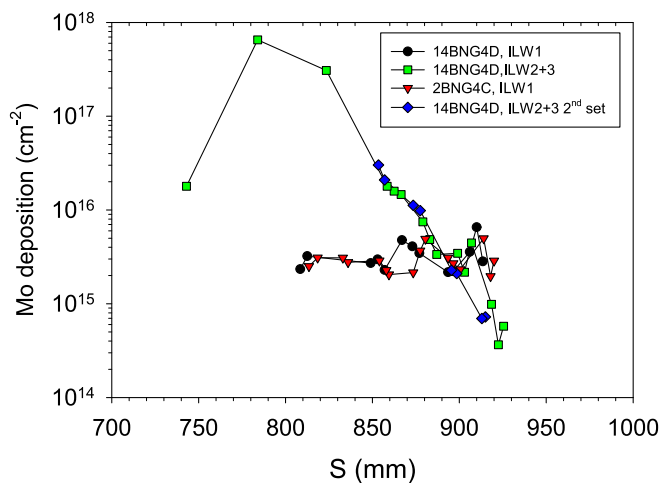


Fig. 6. Normalised SIMS analyses at points on Tiles 14BNG4D and 2BNG4C after exposure during ILW1 and on the replacement Tile 14BNG4D exposed for ILW2 and 3 (in two toroidal locations).

or some mechanism for transfer from the outer divertor through the private region to the inner divertor. Given these transport difficulties and that the erosion from 2BNG4C is  $\sim 50$  times higher than the source from LBO, the contribution of LBO can be regarded as negligible.

The analysis programmes on the tiles and other samples that have been removed from JET at every shutdown since the first one in 1984 have concentrated on the deposition (and to a more limited extent the erosion) of plasma impurities such as carbon (C) and beryllium (Be) within the torus and the retention of the fuelling gas (deuterium). This has led to new understandings of transport mechanisms (e.g. scrape-off layer (SOL) drift), main chamber interactions and re-erosion kinetics being proposed [10] and incorporated into experimental data [1–3]. However, less progress has been made on transport within the divertor where a number of mysteries remain [11]. This data on the erosion and migration of a heavy metal (Mo) within the JET divertor may provide some further input for modelling.

## Conclusions

The JET divertor since 2010 has comprised mostly W-coated carbon-fibre reinforced carbon (CFC) tiles, with one toroidal band of bulk W tiles. For each of the three JET ILW campaigns a few special marker tiles have been placed in the divertor. Amongst the W-coated CFC tiles are tiles coated with a  $\sim 3 \mu\text{m}$  layer of Mo with a  $\sim 4 \mu\text{m}$  topcoat of W to monitor W erosion and tiles with just a  $\sim 4 \mu\text{m}$  layer of Mo – the erosion and re-deposition of Mo from these latter tiles is the subject of this paper.

During ILW1 just one Mo marker tile was included in the band of Tiles 3. For most of the pulses during this campaign the ISP was near the top of Tiles 3. After ILW1 the Mo marker tile was removed for analysis and *inter alia* two W-coated Tiles 4 to check for re-deposited Mo. About 7% of the Mo removed from the Tile 3 Mo marker was found on band 4 tiles, with almost identical amounts on tiles on opposite sides of the torus (Fig. 6). The majority of the Mo would have been re-deposited on other (W-coated) Tiles 3, and significant W was re-deposited on the Mo marker from the surrounding tiles, with a poloidal deposition pattern similar to the Mo erosion (Fig. 4), although their precise locations depend on the topography [5].

A fresh Mo marker Tile 3 was inserted in for ILW2 + 3 plus a Mo

marker Tile 4 for ILW2 (after which it was removed for analysis). Tiles 4 removed after ILW3 were measured for Mo re-deposition. The Mo deposition pattern on Tile 4 was quite different to that after ILW1, with much more Mo located towards the corner of the divertor where plasma impurities such as Be are known to accumulate (Fig. 6).

## CRediT authorship contribution statement

**J. Likonen:** Writing – review & editing. **J.P. Coad:** Writing – review & editing. **E. Alves:** Investigation. **N. Catarino:** Investigation. **I. Coffey:** Investigation. **S. Krat:** Investigation. **M. Mayer:** Investigation. **K. Mizohata:** Investigation. **A. Widdowson:** Investigation.

## Declaration of Competing Interest

The authors declare that they have no known competing financial interests or personal relationships that could have appeared to influence the work reported in this paper.

## Data availability

No data was used for the research described in the article.

## Acknowledgements

This work has been carried out within the framework of the EURO-fusion Consortium, funded by the European Union via the Euratom Research and Training Programme (Grant Agreement No 101052200 – EUROfusion), from the EPSRC [grant number EP/W006839/1]. Views and opinions expressed are however those of the author(s) only and do not necessarily reflect those of the European Union or the European Commission. Neither the European Union nor the European Commission can be held responsible for them. The research used UKAEA's Materials Research Facility, which has been funded by and is part of the UK's National Nuclear User Facility and Henry Royce Institute for Advanced Materials.

## References

- [1] J.P. Coad, M. Rubel, J. Likonen, N. Bekris, S. Brezinsek, G.F. Matthews, M. Mayer, A.M. Widdowson, *Fus. Eng. Design* 138 (2019) 78–108.
- [2] A. Widdowson, J.P. Coad, Y. Zayachuk, et al., *Physica Scripta* 96 (2021), 124075.
- [3] S. Krat, M. Mayer, A. Baron-Wiechec, S. Brezinsek, P. Coad, K. Yu Gasparyan, I. Heinola, J. Jepu, P. Likonen, C. Petersson, G. de Ruset, A.W. Saint-Aubin, *Physica Scripta* T171 (2020), 014059.
- [4] A. Lahtinen, J. Likonen, S. Koivuranta, A. Hakola, K. Heinola, C.F. Ayres, A. Baron-Wiechec, J.P. Coad, A. Widdowson, J. Räisänen, *Nucl. Mater. Energy* 12 (2017) 655.
- [5] M. Tokitani, M. Miyamoto, S. Masuzaki, R. Sakamoto, Y. Oya, T. Hatano, T. Otsuka, M. Oyaizu, H. Kurojaki, T. Suzuki, D. Hamaguchi, K. Isobe, N. Asakura, A. Widdowson, K. Heinola, M. Rubel, *Fus. Eng. Design* 136 (2018) 199.
- [6] W. Eckstein, *Topics in Applied Physics* 10 (2007) 33–187.
- [7] S. Brezinsek, S. Wiesen, D. Harting, C. Guillemaut, A.J. Webster, K. Heinola, A. G. Meigs, M. Rack, Y. Gao, G. Sergienko, *Physica Scripta* T167 (2016), 014076.
- [8] T. Nakano, A.E. Shumack, C.F. Maggi, et al., *Journal of Physics B: Atomic, Molecular and Optical Physics* 48 (2015), 144023.
- [9] I. Coffey private communication.
- [10] J.P. Coad, P.L. Andrew, J.D. Elder, S.K. Erents, H.Y. Guo, C.F. Maggi, G.F. Matthews and P.C. Stangeby, 26<sup>th</sup> EPS Conf. on Controlled Fusion and Plasma Physics, Maastricht, June 1999.
- [11] A. Widdowson, J.P. Coad, E. Alves, A. Baron-Wiechec, N.P. Barradas, J. Beal, N. Catarino, V. Corregidor, K. Heinola, S. Krat, A. Lahtinen, J. Likonen, G. F. Matthews, M. Mayer, P. Petersson, M. Rubel, *Physica Scripta* T170 (2017), 014060.